Nghiên cứu sự trao đổi và hấp phụ các cation kim loại trên bề mặt kaolinite từ lý thuyết phiếm hàm mật độ

Tóm tắt

Trong nghiên cứu này các quá trình trao đổi và hấp phụ các cation kim loại được khảo sát sử dụng các tính toán theo các nguyên lý đầu tiên. Các kết quả thu được chỉ ra rằng, các sự trao đổi cation hầu như không thuận lợi, trong đó các vị trí Al^{3+} dễ thay thế hơn Si^{4+}. Các cation kim loại được hấp phụ mạnh mẽ trên kaolinite ở cả hai mặt H-slab và O-slab. Kết quả tính tại phiếm hàm PBE, khả năng hấp phụ các cation kim loại giảm theo thứ tự $Li^+ > K^+ > Na^+ > Ca^{2+} > Al^{3+} > Fe^{3+} > Cr^{3+} > Mg^{2+}$. Đáng chú ý, sự xâm nhập vào cấu trúc tinh thể của kaolinite được phát hiện đối với Li^+ và Mg^{2+} ở mặt H-slab cùng với sự hình thành tương ứng các liên kết mới Li-O và Mg-O. Trong khi đó, sự xen vào giữa các lớp kaolinite bởi các cation Ca^{2+} được phát hiện với sự hình thành các liên kết Ca-O với cả hai mặt H-slab và O-slab. Đối với Na^+, K^+, hay Cr^{3+}, sự ưu tiên ở bề mặt O-slab trong quá trình hấp phụ. Trong khi đó, Al^{3+} và Fe^{3+} tạo sự tương tác tốt ở trên bề mặt H-slab. Các phân tích mật độ trạng thái và phân bố mật độ electron chứng tỏ sự hình thành các liên kết cộng hóa trị M-O trong quá trình hấp phụ. Hơn nữa, K^+ được đề xuất như là sự bổ sung trên bề mặt kaolinite đối với các khảo sát xa hơn về hấp phụ và loại bỏ hiệu quả các hợp chất hữu cơ trong các môi trường.

Từ khóa: *Sự trao đổi, hấp phụ, cation kim loại, kaolinite, DFT.*

Metal cation exchange and adsorption onto kaolinite surfaces: A DFT study

Abstract

In this study, metal cations exchange and adsorption processes onto kaolinite surfaces are investigated using first-principles calculations. Obtained results indicate that the exchanges of cations are mostly unfavorable, and the Al sites are conveniently replaced compared to Si sites. The metal cations are adsorbed strongly onto kaolinite surfaces at both O-slab and H-slab. The adsorption ability of metal cations decreases in the order of $Li^+ > K^+ > Na^+ > Ca^{2+} > Al^{3+} > Fe^{3+} > Cr^{3+} > Mg^{2+}$ at the PBE functional. Remarkably, the insertions of Li^+ and Mg^{2+} into the lattice structure of kaolinite are found at H-slab following the formation of Li-O and Mg-O new bonds, respectively. While the intercalation into kaolinite by Ca^{2+} is observed in forming Ca-O bonds with both H-slab and O-slab. For Na^+, K^+, and Cr^{3+}, the favorable attachment is located at the O-slab upon adsorption. Besides, the Al^{3+} and Fe^{3+} ions interact preferably on the H-slab. The analyses of the density of states and electron localization function clarify the appearance of M-O covalent bonds upon the adsorption process. Further, K^+ is suggested as a promising addition to kaolinite surfaces for the efficient adsorption and removal organic compounds in environments.

Keywords. *Exchange, Adsorption, Metal cations, Kaolinite, DFT.*

1. INTRODUCTION

Kaolinite is one of two-layer aluminosilicates, containing the hydrogen-rich surface (H-slab) and oxygen-rich surface (O-slab). The H-slab with high positive charge density is favorable for interaction with organic compounds containing functional groups such as -OH, -COOH.[1-3] In particular, the adsorptions of benzene, n-hexane, pyridine, and 2-propanol on H-slab are more substantial than those on O-slab.[4] Similarly, phenol, toluene, and CO_2 are adsorbed preferably on the kaolinite aluminol surface (H-slab).[5] In contrast, the O-slab containing a sizeable negative charge density is considered an efficient surface for the adhesion of metal cations or other cations.[6-8] As a result, kaolinite is one of the potential materials for the adsorption and removal of heavy metals from aquatic environments.[9] Besides, theoretical approaches using density functional theory (DFT) provide insight into the adsorption process of metal cations on material surfaces.[1-8]

It is noticeable that the exchange of cations in the material structure leads to considerable changes in electronic and surface properties, increasing the applicability of materials, especially in energy and environment fields.[10] Recently, the alkali activated kaolinite has been investigated for antibiotic adsorption.[11] Accordingly, replacing Al^{3+}/Si^{4+} on kaolinite with Na^+ cations improves adsorption performance. In another report, the hydrated form of Cd(II) adsorbed on basal planes of kaolinite (H-slab and O-slab) was carried out using theoretical approach.[12] Moreover, Cs(I) adsorption on kaolinite was more convenient for O-slab than for H-slab.[13] It can be seen that the hydrated forms of metal cations and material surfaces in aquatic environments are quite complex, affected by various factors such as temperature, pressure, concentration, pH, and the presence of other compounds. Additionally, the suitable planar surface of kaolinite for the cation adsorption was not clarified in the previous studies. Therefore, in the present work, we use DFT calculations to investigate the replacement of exchangeable cations in the structure of kaolinite (Al^{3+}, Si^{4+}), and adsorption of various cations with the unhydrated form on both H-slab and O-slab, to have an insight into the structural and electronic properties, surface interactions. Furthermore, results are expected to suggest promising metal cations adding to the kaolinite surface for the good adsorption and removal of organic pollutants in environments.

2. COMPUTATIONAL METHOD

The geometric structures of the kaolinite surfaces and adsorption configurations are optimized by VASP.[14] Kaolinite is one of the common clay minerals, including a series of uncharged layers connected by a network of hydrogen bonds between H-slab and O-slab, as shown in Figure 1. In this work, the *1 x 1 x 1* (for one layer in exchange) and *2 x 1 x 1* (for two layers in adsorption) cell models are designed with dimensions size of the unit cell in experiments[15]: a = 5.15 Å; b = 8.93 Å; c = 7.38 Å, and a = 10.30 Å; b = 8.93 Å; c = 28.51 Å, respectively. The vacuum

space in the two-layered structure is 15 Å, large enough to ignore boundary interactions between two slabs. Plane-wave cutoff energy is set up at 500 eV upon optimization.

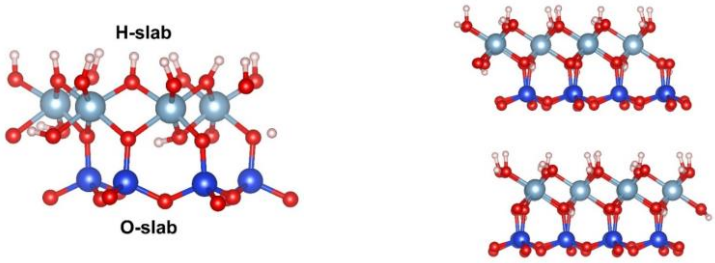

One layer (unit cell) **Two layers**

Figure 1. The surface models of kaolinite in this work

In addition, the Perdew-Burke-Ernzerhof (PBE) function with a generalized gradient approximation (GGA) for the exchange-correlation component is used in all calculations.[16] Adsorption energy (E_{ads}) is computed by using the following expressions:

$$E_{ads} = E_{comp} - E_{kaoli} - E_M$$

where E_{comp}, E_{kaoli} and E_M are the energy values of complexes, kaolinite surfaces, and metal cations, respectively. The exchange energy (E_{exh}) of metal cations into the lattice structure of kaolinite is determined as follows:

$$E_{exh} = E_{kaoli\text{-}M} + E_{Al/Si} - E_M - E_{kaoli}$$

in which $E_{kaoli\text{-}M}$ and $E_{Al/Si}$ correspond to the energy values of the new structure of cation exchange and Al^{3+}/Si^{4+}. Moreover, to understand the formation of stable structures, the density of states (DOS) and electronic localization function (ELF) analyses are carried out at the same level of theory.

3. RESULTS AND DISCUSSION

3.1. Optimized structures

The stable configurations of exchange and adsorption of metal cations (M), including Li^+, Na^+, K^+, Mg^{2+}, Ca^{2+}, Al^{3+}, $Cr^{3+,}$ and Fe^{3+} based on DFT calculations at PBE functional, are presented in Figures 2 and 3. Accordingly, the cation exchange occurs at Al^{3+} or Si^{4+} sites of kaolinite lattice structure. Some Al-O or Si-O bonds are broken and replaced by new M-O bonds upon optimization. The bond lengths of Al/Si-O in kaolinite are ca. 1.85-2.00 Å (Al) and 1.61-1.64 Å (Si), consistent with experiment values in previous studies.[17]

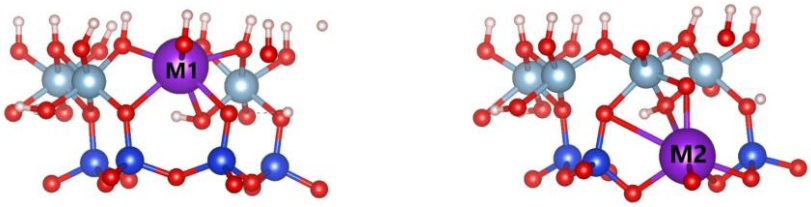

Exch-M1 (at Al site) **Exch-M2 (at Si site)**

Figure 2. The optimized structures of cations exchange on kaolinite surfaces

For derivatives in exchange, the M-O bond lengths for replacement of Al^{3+} (denoted by M1) and Si^{4+} (denoted by M2) sites are 1.97-2.24 Å (Li1), 1.80-1.89 Å (Li2), 2.13-2.37 Å (Na1), 2.08-2.17 Å (Na2), 2.35-2.89 Å (K1), 2.30-3.15 Å (K2), 1.99-2.07 Å (Mg1), 1.86-1.92 Å (Mg2), 2.18-2.30 Å (Ca1), 2.11-2.73 Å (Ca2), 1.73-1.75 Å (Al2), 1.84-1.99 Å (Si1), 1.91-2.03 Å (Cr1), 1.72-1.80 Å (Cr2), 1.88-2.01 Å (Fe1), 1.73-1.81 Å (Fe2). As a result, the M-O distances are larger at M2 than at M1 structures following the cation exchange. Moreover, the charge densities surrounding Al/Si sites in kaolinite change in replacing metal cations. Hence, the cation substitutions lead to considerable changes in M-O bond length and charge density on M, which could cause a decrease in structure strength compared to original kaolinite.

In addition, the adsorption of metal cations onto kaolinite is observed at the H-slab, O-slab, and between two of these slabs, as displayed in Figure 3. According to the optimization, metal cations attach on H-slab at the O sites to form M-O interactions in **Ads-M1**, while the adhesion of metal cations on O-slab is preferred at the tetragonal cage in **Ads-M3** and hexagonal cage in **Ads-M4**. The attachment of cations into the interlayer of H-slab and O-slab is considered in the

present work. Here, the configurations are stabilized by M-O new bonds in **Ads-M2**.

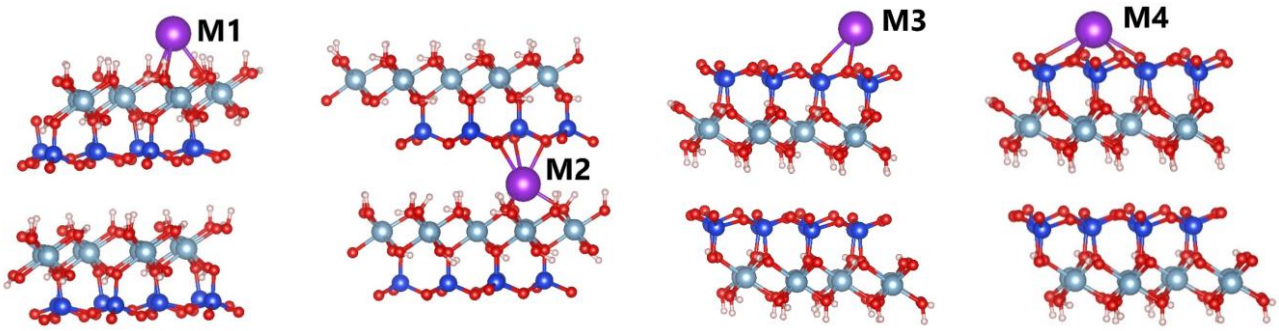

Figure 3. The stable structures of cations adsorption on kaolinite surfaces.

The interaction distances in adsorption configurations (**Ads-M1**, **Ads-M2**, **Ads-M3**, **Ads-M4**) are mostly larger than M-O bond lengths in cation exchange. In particular, the M-O distances are ca. 2.66-2.69 Å (Li1), 2.04-2.29 Å (Li2), 1.90-2.57 Å (Li3), 2.08-2.50 Å (Li4), 2.45-2.50 Å (Na1), 2.27-2.90 Å (Na2), 2.35-2.66 Å (Na3), 2.39-2.95 Å (Na4), 2.80-2.82 Å (K1), 2.49-3.02 Å (K2), 2.65-3.06 Å (K3), 2.75-3.14 Å (K4), 2.22 Å (Mg1), 2.05-2.14 Å (Mg2), 2.92 Å (Mg3), 3.25 Å (Mg4), 2.42 Å (Ca1), 2.32-2.73 Å (Ca2), 2.40 Å (Ca3), 2.47-2.50 Å (Ca4), 2.01 Å (Al1), 2.14-3.08 Å (Al2), 2.16 Å (Al3), 2.31-2.94 Å (Al4), 2.50-2.65 Å (Cr1), 2.13-3.02 Å (Cr2), 2.27 Å (Cr3), 2.28 Å (Cr4), 2.38-2.69 Å (Fe1), 1.97-3.56 Å (Fe2), 2.23 Å (Fe3), 2.45-2.92 Å (Fe4) upon adsorptions. Noticeably, the Li^+ and Mg^{2+} cations tend to insert into the lattice structure of kaolinite and form Li-O and Mg-O new bonds along with Al-O bonds at H-slab.

3.2. Exchange and adsorption energies

The characteristic parameters such as the exchange energy (E_{exh}) and adsorption energy (E_{ads}) calculated and gathered in Table 1 aim to evaluate the exchange and adsorption ability of cations onto kaolinite surfaces.

Table 1. The energy of cation exchange (E_{exh}) and adsorption (E_{ads}) on kaolinite (in kcal.mol^{-1}).

	M	Li^+	Na^+	K^+	Mg^{2+}	Ca^{2+}	Al^{3+}	Cr^{3+}	Fe^{3+}
E_{exh}	**Exch-M1**	214.7	250.0	282.5	126.1	123.2	--	**57.7**	96.6
	Exch-M2	284.5	326.5	357.6	210.9	210.6	**70.9**	92.3	132.8
E_{ads}	**Ads-M1**	-12.9	-12.1	-12.7	-5.5	-11.8	**-22.6**	-6.7	**-11.7**
	Ads-M2	**-61.9**	-25.9	-14.6	**-7.0**	**-24.3**	-12.0	-6.7	-10.5
	Ads-M3	-26.8	-21.4	-25.3	-0.7	-14.2	-18.1	-7.9	-8.1
	Ads-M4	-42.1	**-29.8**	**-33.5**	-0.8	-21.6	-17.4	**-8.7**	-7.1

Calculated results show that the exchange energy values are highly positive, in the range of 57.7-357.6 kcal.mol^{-1}, indicating these processes are endothermic and thermodynamically unfavorable. This result is consistent with the previous report on substitutions in kaolinite by combining ions from groups II and III.[18] As a result, the replacement of Al^{3+}/Si^{4+} with Cr^{3+}, and Fe^{3+} are more convenient than other cations. The cation exchanges are more favorable at the Al^{3+} than at Si^{4+}, especially the Cr-derivative (E_{exh} ca. 57.7 kcal.mol^{-1}). With the Si^{4+} substitutions, the Al-derivative (E_{exh} ca. 70.9 kcal.mol^{-1}) is formed more preferably than other ones. Here, it can be understood that the changes in charge density and radius of the metal cations yield changes in geometrical structures. The substituted metal cations mostly have a smaller charge and a much different radius than the substituted Al^{3+}/Si^{4+} in kaolinite, leading to the formation of less stable structures.

Considering the adsorption of metal cations onto H-slab and O-slab, the adsorption energy (E_{ads}) ranges from -7.0 to -61.9 kcal.mol^{-1}. The obtained configurations are thus relatively stable. The metal cations are adsorbed strongly to different sites onto kaolinite surfaces. Specifically, Li^+ cations tend to insert into the kaolinite in the octahedral cage and form Li-O new bonds in the **Ads-Li2** (E_{ads} = -61.9 kcal.mol^{-1}), the most stable structure in investigated systems. The **Ads-Li4** is formed conveniently with an adsorption energy value of -42.1 kcal.mol^{-1}, and Li-O bonds located at the octahedral cage of the O-slab. This is due to

the Li^+ ion has the smallest radius among the investigated cations, so it is conveniently located at cages of H-slab and O-slab and inserted into the lattice structure of kaolinite. Besides, Na^+, K^+, and Cr^{3+} cations interact considerably with O sites on the O-slab in forming the **Ads-Na4**, **Ads-K4,** and **Ads-Cr4** with corresponding adsorption energies of -29.8, -33.5, and -8.7 kcal.mol^{-1}. These structures are much more stable than **Ads-Na1**, **Ads-K1**, and **Ads-Cr1** where the adsorption occurs preferably on the H-slab.

In addition, the Al^{3+} and Fe^{3+} cations are adsorbed strongly at the H-slab leading to the existence of M-O bonds at the top of the tetrahedral cage in **Ads-Al1** (E_{ads} of - 22.6 kcal.mol^{-1}) and **Ads-Fe1** (E_{ads} of -11.7 kcal.mol^{-1}). These configurations are about 4-5 kcal.mol$^{-1,}$ more stable than **Ads-Al4** and **Ads-Fe4**. With the remaining metal cations (Mg^{2+}, Ca^{2+}), the most stable configurations are **Ads-Mg2** and **Ads-Ca2** with the intercalation of ions between the H-slab and O-slab. Here, Mg^{2+} inserts into the H-slab and forms Mg-O bonds similar to Li^+. However, the **Ads-Mg2** (E_{ads} of -7.0 kcal.mol^{-1}) is much less stable than **Ads-Li2**. Meanwhile, the intercalation of Ca^{2+} yields the appearance of Ca-O bonds with both H-slab and O-slab. The **Ads-Ca2** is thus relatively stable in this case, with an adsorption energy of -24.3 kcal.mol^{-1}. Furthermore, results indicate that among the common metal cations in aqueous environments (Na^+, K^+, Mg^{2+}, and Ca^{2+}), K^+ has the best adsorption ability on kaolinite surfaces. In previous reports, the alkali metal (Na, Mg, Ca) supported on kaolinite enhances the adsorption capacity of heavy metal.[19,20] From this aspect, K^+ is expected to be a good candidate to support kaolinite surfaces for the adsorption of heavy metals and organic compounds.

3.3. DOS and ELF analyses

To better understand the formation of structures following the exchange and adsorption of cations, the density of states (DOS) and electron localization function (ELF) analyses at the PBE function are examined and illustrated in Figures 4 and 5.

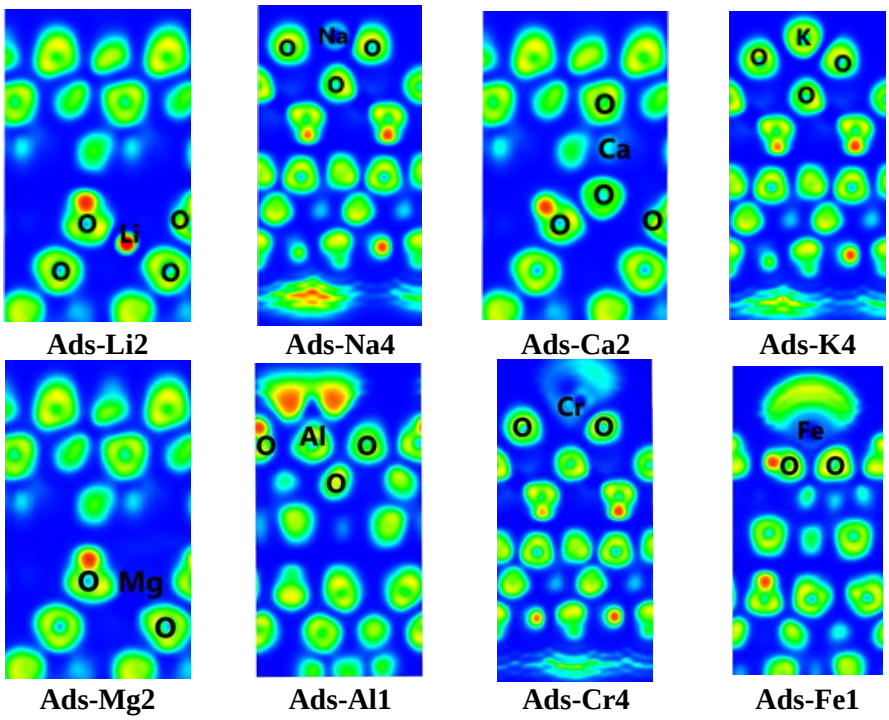

Figure 4. The ELF maps of the most stable adsorption configurations.

Results of ELF analysis indicate that the interactions are formed between M metals and O at the H-slab and O-slab with highly localized electron density, regarded as the chemical bonds.[21] The electron density sharing between M-O bonds is more favorable at the O-slab surface than at the H-slab. Moreover, the electron density localized at the M-O bonds for the structures is considerably high and decreases from **Ads-Li2**, **Ads-K4**, and **Ads-Na4**, going to **Ads-Ca2**, **Ads-Al1**, and finally in **Ads -Fe1**, **Ads-Cr4**, **Ads-Mg2**. Therefore, the formation of M-O covalent bonds is preferred in the order of Li, K, Na > Ca, Al > Fe, Cr, and Mg, consistent with the difference in adsorption energy values above.

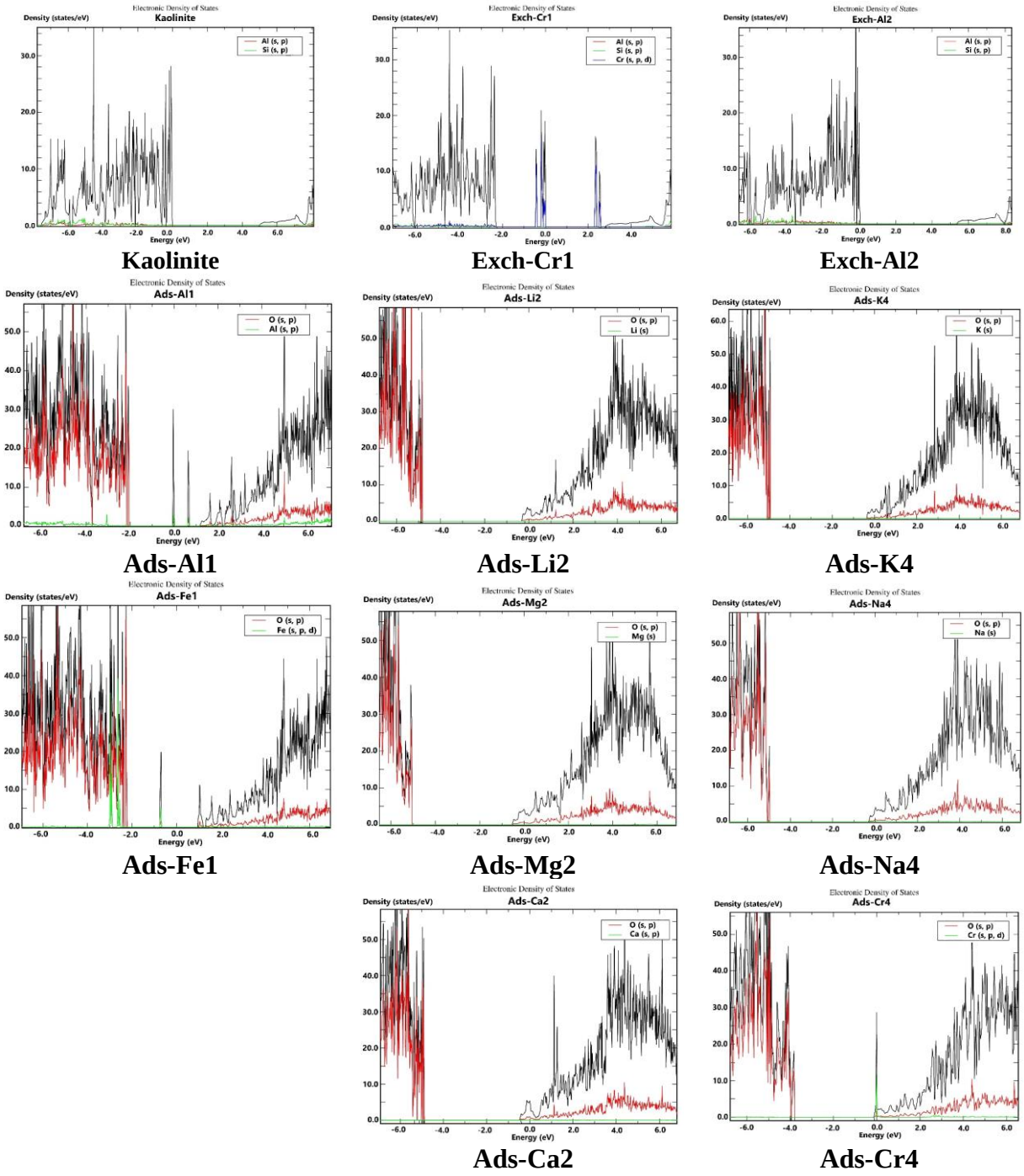

Figure 5. The pDOS of the most stable configurations for metal cations exchange and adsorption

As shown in Fig.5, there are slight decreases in the density of states (DOS) in the valence band (VB) and conduction band (CB). These two shifts are approximate in most structures, so the gap energy (E_g) has little change compared to the initial kaolinite. Besides, in the exchange of Cr^{3+} at Al site (**Exch-Cr1**) and adsorption of Al^{3+}, Fe^{3+} on H-slab (**Ads-M1**), the hybridizations of the 3s, 3p (Al), 3d (Cr, Fe) orbitals and the 2s, 2p orbitals of O (in kaolinite) lead to form Al-O and Cr/Fe-O new bonds. It can be seen from new states as narrow lines between VB and CB. The band gaps of these structures are thus significantly reduced. Therefore, the Cr^{3+} exchange at the Al site and the Al^{3+}, Fe^{3+} adsorption at the H-slab would yield better light absorption and increase the photocatalytic activity of the materials compared to the original kaolinite.

4. CONCLUSIONS

Theoretical results indicate that the cation exchanges into the lattice structure of kaolinite are

unfavorable and endothermic. The adsorption of metal cations on planes of kaolinite is preferred on both H-slab and O-slab in forming M-O bonds. The Li^+, Mg^{2+}, and Ca^{2+} cations are adsorbed alternately to the H-slab and O-slab, in which Li^+ and Mg^{2+} favorably insert into the lattice structure of kaolinite. The Na^+, K^+, and Cr^{3+} ions interact strongly with O sites on the O-slab at the octahedral cage. In addition, Al^{3+} and Fe^{3+} are located firmly at the tetrahedral cage on the H-slab. Adsorptions of metal cations on kaolinite are regarded as chemisorption and follow the sequence: $Li^+ > K^+ > Na^+ > Ca^{2+} > Al^{3+} > Fe^{3+} > Cr^{3+} > Mg^{2+}$. The formation of configurations yields the changes in VB and CB regions and band gap energy. Noticeably, the considerable differences in DOS and band gaps are found in structures of Cr^{3+} exchange and Al^{3+}, Fe^{3+} adsorption as compared to the remaining cations. Besides, the ELF analysis determines the formation of the M-O covalent bonds, which contribute mainly to the stability of configurations.

Acknowledgment. *This research is conducted within the framework of science and technology projects at the institutional level of Quy Nhon University under the project code T2023.797.07.*

REFERENCES

1. R. G. Harris, J. D. Wells, B. B. Johnson. Selective adsorption of dyes and other organic molecules to kaolinite and oxide surfaces, *Colloids Surfaces A Physicochem. Eng. Asp*, **2001**, *180*, 131–140.
2. J. Chen, F. F. Min, L. Liu, C. Liu, F. Lu. Experimental investigation and DFT calculation of different amine/ammonium salts adsorption on kaolinite, *Appl. Surf. Sci*, **2017**, *419*, 241–251.
3. S. Zhang, J. J. Sheng, Z. Qiu. Water adsorption on kaolinite and illite after polyamine adsorption, *J. Pet. Sci. Eng*, **2016**, *142*, 13–20.
4. E. R. Johnson and O. D. L. R. Alberto. Adsorption of organic molecules on kaolinite from the exchange-hole dipole moment dispersion model, *Journal of Chemical Theory and Computation*, **2012**, *8*, 5124-5131.
5. J. Lain, Y. Foucaud, A. Bonilla-Petriciolet, M. Badawi. Molecular picture of the adsorption of phenol, toluene, carbon dioxide and water on kaolinite basal surfaces, *Applied Surface Science*, **2022**, *585*, 152699.
6. L. Liu, F. Min, J. Chen, F. Lu, L. Shen. The adsorption of dodecylamine and oleic acid on kaolinite surfaces: Insights from DFT calculation and experimental investigation, *Applied Surface Science*, **2019**, *470*, 27.
7. F. Fang, F. Min, L. Liu, J. Chen, B. Ren, C. Liu. Adsorption of $Al(OH)_n^{(3-n)+}$ (n = 2–4) on Kaolinite (001) Surfaces: A DFT study, *Applied Clay Science*, **2020**, *187*, 10545.
8. H. Wu, Y. Miao, Y. Li, H. Yan, J. Tan, S. Qiu, H. Wu and T. Qiu. Density Functional Theory Study on the Adsorption of $Fe(OH)_{2+}$ on Kaolinite Surface in Water Environment, *Processes*, **2023**, *11*, 38.
9. X. Wang, Y. Huang, Z. Pan, Y. Wang, C. Liu. Theoretical investigation of lead vapor adsorption on kaolinite surfaces with DFT calculations, *Journal of Hazardous Materials*, **2015**, *295*, 43-54.
10. D. J. Groenendijk and J. N. M. Wunnik. Surfactant Adsorption and Ion Exchange on Calcite Surfaces, *Energy Fuels*, **2021**, *35*, 8763−8772.
11. A. F. A. Majid, R. Dewi, N. N. M. Shahri, E. W. E.S. Shahrin, E. Kusrini, N. Shamsuddin, J.-W. Lim, S. Thongratkaew, K. Faungnawakij, A. Usman. Enhancing adsorption performance of alkali activated kaolinite in the removal of antibiotic rifampicin from aqueous solution, *Colloids and Surfaces A: Physicochemical and Engineering Aspects*, **2023**, *676*, 132209.
12. G. Chen, H. Zhao, X. Li, S. Xia. Theoretical insights into the adsorption mechanism of Cd(II) on the basal surfaces of kaolinite, *Journal of Hazardous Materials*, **2022**, *422*, 126795.
13. Zhongcun Chen, Yaolin Zhao, Dayin Tong, Shaowei Nie, Yuqi Wang, Xiaomeng Nie, Ziqi Jia. A theoretical study of Cs(I) adsorption on kaolinite basal surfaces, *Chemical Physics*, **2022**, *553*, 111380.
14. J. Hafner. Ab-initio simulations of materials using VASP: Density-functional theory and beyond, *Journal of Computational Chemistry*, **2008**, *29*(13), 2044-2078.
15. R. A. Young and A. W. Hewat. Verification of the triclinic crystal structure of kaolinite, *Clays and Clay Minerals*, **1988**, *36(3)*, 225-232.
16. P. Perdew, K. Burke. Generalized gradient approximation made simple, *Phys. Rev. Lett.*, **1996**, *77*, 3865–3868.
17. C. E. White, J. L. Provis, T. Proffen, D. P. Riley, and J. S. J. Deventer. Density Functional Modeling of the Local Structure of Kaolinite Subjected to Thermal Dehydroxylation, *J. Phys. Chem. A*, **2010**, *114*, 4988–4996.
18. M.-C. He, J. Zhao, Z.-J. Fang, and P. Zhang. First-principles study of isomorphic ('dual-defect') substitution in kaolinite, *Clays and Clay Minerals*, **2011**, *59(5)*, 501–506,.
19. J. Luo, H. Yi, J. Wang, Z. Wang, B. Shen, J. Xu, L. Liu, Q. Shi, C. Huang. Effect of alkaline metals (Na, Ca) on heavy metals adsorption by kaolinite during coal combustion: Experimental and DFT studies, *Fuel*, **2023**, *348*, 128503.
20. G. Chen, X. Li, H. Zhao, M. Qiu, S. Xia, L. Yu. Revealing the mechanisms of mercury adsorption on metal-doped kaolinite (001) surfaces by first

principles, *Journal of Hazardous Materials*, **2022**, *431*, 128586.

21. K. Koumpouras and J. A. Larsson. Distinguishing between chemical bonding and physical binding using electron localization function (ELF), *J. Phys.: Condens. Matter*, **2020**, *32*, 315502 (1-12).